

Deep Ordinal Regression using Optimal Transport Loss and Unimodal Output Probabilities

Uri Shaham^{1*}, Jonathan Svirsky

¹Yale University

uri.shaham@yale.edu, jonathan.svirsky@gmail.com

Abstract

We propose a framework for deep ordinal regression, based on unimodal output distribution and optimal transport loss. Despite being seemingly appropriate, in many recent works the unimodality requirement is either absent, or implemented using soft targets, which do not guarantee unimodal outputs at inference. In addition, we argue that the standard maximum likelihood objective is not suitable for ordinal regression problems, and that optimal transport is better suited for this task, as it naturally captures the order of the classes. Inspired by the well-known Proportional Odds model, we propose to modify its design by using an architectural mechanism which guarantees that the model output distribution will be unimodal. We empirically analyze the different components of our proposed approach and demonstrate their contribution to the performance of the model. Experimental results on three real-world datasets demonstrate that our proposed approach performs on par with several recently proposed deep learning approaches for deep ordinal regression with unimodal output probabilities, while having guarantee on the output unimodality. In addition, we demonstrate that the level of prediction uncertainty of the model correlates with its accuracy.

1 Introduction

Ordinal regression is an area of supervised machine learning, where the goal is to predict the value of a discrete dependent variable, whose set of (symbolic) possible values is ordered. Despite often overshadowed by more common applications like classification and regression, ordinal regression covers a wide range of important applications, such as prediction of failure times, ranking, age estimation and many more.

Many practitioners often treat ordinal regression problems as classification or regression problems (for example, this was indeed the case with many submissions to Kaggle’s Diabetic Retinopathy competition¹ in 2015). While having common

characteristics with both classification and regression, ordinal regression can arguably be viewed a mid-point between the two. An ordinal model is of course similar to a classification model, as both predict a discrete value (“label”) out of a finite set of possible ones. However, the existence of an order on set of labels, when available, can potentially lead to an improved performance, comparing to a standard classifier, which does not assume such order. This typically occurs via distinguishing between the severity of prediction mistakes: while in classification typically “all mistakes are created equal”, in ordinal regression different mistakes may be associated with different severity (for example, predicting “moderately-sized” when the ground truth value is “big” may be less severe than a “tiny” prediction. In regression problems, the dependent variable naturally does take values from an ordered set. However, this set is typically a continuum. Moreover, regression performance may be sensitive to monotonic transformations of the dependent variable, while such sensitivity does not take place in ordinal regression problems. Hence one may expect that typical ordinal regression algorithms have potential to outperform classification or regression approaches, when the range of the dependent variable is finite and ordered. In section 5 we will provide examples to the superiority of our proposed approach over classification and regression in benchmark tasks.

The arguably most fundamental ordinal regression model is the Proportional Odds Model (POM), a generalized linear model, similar in spirit to logistic regression, however where the logits are defined for cumulative probabilities. POM is typically trained via maximum likelihood (as is also the case for several recently proposed deep ordinal regression approaches, which will be reviewed in section 2). We argue that likelihood is a sub-optimal measure of optimality for ordinal regression setup, as it only considers the probability mass the model assigns to the true class, ignoring the remaining mass. This implicitly assumes that “all mistakes are equal”, which, as discussed above, is not the case for ordinal regression. Hence we seek for an alternative measure of quality which may be more appropriate for ordinal regression. We argue that the optimal transport divergence might be a better fit. In addition, this divergence turns out to be particularly appealing, as it obtains a simple, differentiable form in the case that one of the distributions is Dirac, which is indeed the case in ordinal regression; this will be explained in Section 3.

*Contact Author

¹<https://www.kaggle.com/c/diabetic-retinopathy-detection/>

Another potential source of sub-optimality of POM (and of several recently-proposed approaches for deep ordinal regression) is the reasonable requirement that a probabilistic model for ordinal regression will output unimodal probabilities (i.e., that when moving in either direction from the most probable class, the probabilities predicted by the model will decay in a monotonic fashion. Despite being a natural requirement, it is unfortunately not always fulfilled. While this was identified by several recent works for deep ordinal regression, unimodality is often encouraged via soft targets. In section 2, we will argue that this is a sub-optimal means to achieve unimodality. To the contrary, we propose a novel mechanism to enforce unimodality of the output distribution, implemented via architectural design, and demonstrate that it does not hurt the level of performance.

Experimentally, we analyze the contribution of the optimal transport objective and our proposed unimodality mechanism to the performance of the model, and provide results on three real world vision benchmarks which demonstrate that our proposed approach performs on par with several recently proposed approaches for deep ordinal regression, while having a unimodality guarantee. In addition, we demonstrate that the output probabilities correspond to the level of uncertainty of the model in its predictions.

2 Related Work

Several deep learning approaches for ordinal regression were proposed in the recent years. A common approach seems to be to turn the ordinal regression problem into a multi-label classification problem, for example [Fu *et al.*, 2018; Liu *et al.*, 2017, 2018b; TV *et al.*, 2019; Berg *et al.*, 2020; Cheng *et al.*, 2008]. We argue that the multi-label approach has two major problematic aspects: first, the output probabilities are not always guaranteed to be consistent, in the sense of decreasing cumulative distribution (that is we would like to predict $\Pr(y \geq 1) \geq \Pr(y \geq 2) \geq \dots \geq \Pr(y \geq k)$). Second, even if the output probabilities are consistent, as is the case in [Liu *et al.*, 2018a] for example, the predicted class probabilities are not necessarily unimodal, i.e., there is no guarantee for existence of $j \in \{1, \dots, k\}$ such that $\Pr(Y = 1) \leq \dots \leq \Pr(Y = j) \geq \dots \geq \Pr(Y = k)$. The component of unimodal output probabilities is also lacking in [Liu *et al.*, 2019b] and [Vargas *et al.*, 2020], which both propose probabilistic approaches employing learned thresholds of the real line, as well as in [Pan *et al.*, 2018].

Beckham and Pal [2017] proposed an elegant mechanism to obtain unimodal output probabilities, based on either the Poisson or the Binomial distributions, which are both unimodal. In both cases their model outputs a scalar (λ in case of the Poisson, p in the case of the binomial), which is then mapped to a probability mass function that uses (after normalization) as the model output probabilities. While being a convenient, architectural-based solution for the unimodality issue, their approach is inherently limited in its ability to express the level of uncertainty of the model’s prediction: since a single parameter determines both the location of the mode, and the decay of the probabilities, the model cannot output a highly flat or highly peaked probability vector; in addition,

instances of the same predicted class ought to have similar output probabilities. Inspired by their approach, we utilize the normal distribution, in which one parameter determines the location while another determines the decay. In section 5 we will demonstrate that this greater flexibility yields an improvement in performance. Belharbi *et al.* [2019] propose a constrained optimization approach to achieve unimodality. However, this comes at a cost of a somewhat cumbersome optimization process. More importantly, even if unimodality is indeed achieved for the train data, there are no guarantees that this will also be the case for unseen test data.

Several works propose to handle the unimodality requirement via soft targets, for example [Gao *et al.*, 2017; Diaz and Marathe, 2019; Liu *et al.*, 2019a, 2020]. We argue that the usage of soft targets to obtain unimodality is sub-optimal, as it does not guarantee unimodal outputs at inference (and not even at train time). We will demonstrate this issue in section 5. In comparison, in our approach the unimodality is guaranteed via architectural design (as is also the case in [Beckham and Pal, 2017]).

Several works propose the training objective to be cross entropy, while using one-hot (or binary) targets, see, for example [Belharbi *et al.*, 2019], [Vargas *et al.*, 2020], Fu *et al.* [2018]; Beckham and Pal [2017]; Berg *et al.* [2020]; TV *et al.* [2019]. As pointed out in several papers, and will also be demonstrated in section 3, in the case of one-hot targets, the cross entropy term equals the negative log of the probability assigned by the model to the true class, making it invariant to the distribution of the remaining probability mass. While a reasonable thing in a standard classification setting, this ignores the ordering of the classes, making it a sub-optimal choice for ordinal regression setting. To overcome this limitation of cross entropy Hou *et al.* [2016], followed by [Beckham and Pal, 2017; Liu *et al.*, 2019a] use optimal transport loss, which is a natural way to incorporate the order of the classes into the loss term. In this sense, it is similar to the approach we take in this manuscript.

To summarize this section, we identify the following requirements for an appropriate ordinal regression model:

- Unimodality of the model’s output distribution.
- It is advantageous to enforce the unimodality via the design of the model, rather than via soft targets.
- A model utilizing one-hot targets should not be trained using cross entropy objective (or maximum likelihood in general).
- The decay of the output probabilities should reflect the uncertainty of the model in its predictions.

These requirements naturally lead us to our proposed approach in section 4. However, before we specify it, we begin with a brief review of the proportional odds model and optimal transport divergence.

3 Preliminaries

We begin this section with a description of the proportional odds model from a latent variable perspective. We then briefly review optimal transport as a divergence between two probability distributions.

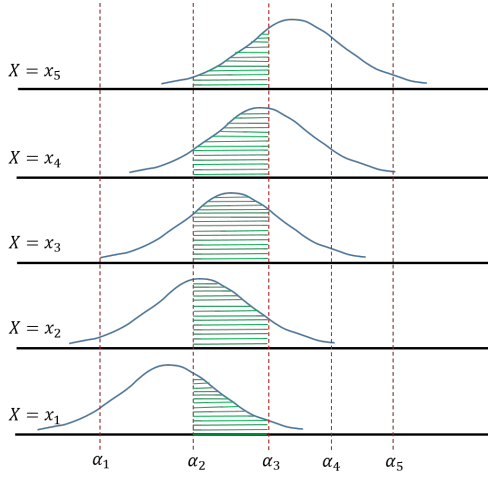


Figure 1: The proportional odds model. x_i is a realization of X . The standard logistic density is shifted by $\beta^T x_i$. The thresholds α_j define the bins which determine the probability predicted by the model to each class. For example, the green area defines the probability $\Pr(Y = 3)$.

3.1 The Proportional Odds Model

Let $(X, Y) \in \mathcal{X} \times \mathcal{Y}$ be random variables, having joint probability \mathcal{P}_{XY} , where $\mathcal{X} = \mathbb{R}^d$ and $\mathcal{Y} = \{1, \dots, k\}$, where $1, \dots, k$ are considered as symbols. Let \preceq be an order relation defined on \mathcal{Y} such that $1 \preceq \dots \preceq k$. The proportional odds model is parametrized by $\alpha \in \mathbb{R}^{k-1}$, $\beta \in \mathbb{R}^d$ and applies to data $\{(x_i, y_i)\}_{i=1}^n$, sampled i.i.d from \mathcal{P}_{XY} .

Let ϵ be a logistic random variable (thus having a sigmoid cumulative distribution function $F(x) = \frac{1}{1+\exp(-x)}$), and let Z be a random variable defined as $Z = \beta^T X + \epsilon$. The entries of α use to define the cumulative conditional probabilities via

$$\Pr(Y \preceq j | X = x) = \Pr(Z \leq \alpha_j) = F(\alpha_j - \beta^T x). \quad (1)$$

Similarly to logistic regression, this yields linear log-odds (logits), however, defined with respect to cumulative terms

$$\gamma_j \equiv \log \frac{\Pr(Y \preceq j | X = x)}{\Pr(Y \succ j | X = x)} = \alpha_j - \beta^T x.$$

It is convenient to interpret equation (1) by viewing $\beta^T x$ as a factor that shifts the standard logistic density function, while the α_j terms are thresholds, with respect to which the cumulative probabilities are defined. This is depicted in Figure 1. Let (x, y) be a realization of (X, Y) . The likelihood assigned by the model to (x, y) is

$$\begin{aligned} L(\alpha, \beta; (x, y)) &= \Pr(Y = y | X = x; \alpha, \beta) \\ &= F(\alpha_y - \beta^T x) - F(\alpha_{y-1} - \beta^T x), \end{aligned} \quad (2)$$

considering $\alpha_0 = -\infty$ and $\alpha_k = \infty$. The model is typically trained in a standard fashion by maximizing the log-likelihood function on the training data.

Despite its popularity, the POM suffers from two main issues: First, the model's output probabilities are not necessarily unimodal. This is depicted in Figure 2. Second, the likeli-

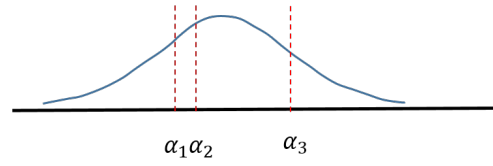


Figure 2: POM does not always output unimodal probabilities. Recall that $\Pr(Y = k) = \Pr(Z \leq \alpha_k) - \Pr(Z \leq \alpha_{k-1})$. Therefore, the above plot shows an example where the output probabilities are such that $\Pr(Y = 1) > \Pr(Y = 2) < \Pr(Y = 3) > \Pr(Y = 4)$ (i.e., the output probabilities are bimodal and not unimodal).

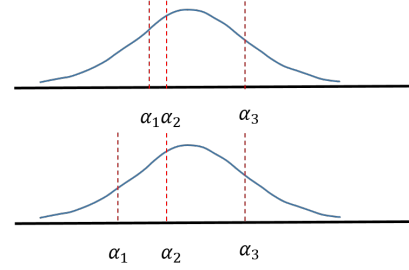


Figure 3: The likelihood function of POM is invariant to the way the predicted probability mass of the incorrect classes is assigned. In the above example the correct class is 3, and the two instances have the same likelihood, despite the fact that in the bottom case, the probability mass assigns to neighboring class 2 is larger, making the bottom case more appropriate than the top one.

hood function (2) only depends on the probability the model assigns to the correct class y , and is invariant to the way the remaining probability mass is assigned by the model. This ignores the order on the label set, and hence does not use important information that might be used to improve prediction quality, as depicted in Figure 3.

It is important to mention that as cross entropy term is essentially equivalent to model's negative log-likelihood function, this invariance to the partition of the remaining mass over the incorrect classes is common to all models trained via cross entropy minimization, as long as the target labels are one-hot.

In section 4 we will show how our method overcomes these two limitations of the POM.

3.2 Optimal Transport

Let (M, d) be a finite metric space, and let p, q be probability mass functions defined on M . Optimal transport, also denoted as the 1-Wasserstein distance and the Earth Mover Distance, between p and q is

$$OT(p, q) = \inf_{\gamma \in \Gamma} \int d(x, y) d\gamma(x, y), \quad (3)$$

where Γ is the set of all joint probabilities on $M \times M$, having marginals p and q , and the metric d specifies the costs of moving probability mass between every two elements of M . This amounts to the optimal transportation of probability mass that transforms p into q and vice versa. In the general case, the distance can be found by solving a linear program, and several relaxations have been proposed to accelerate its computations

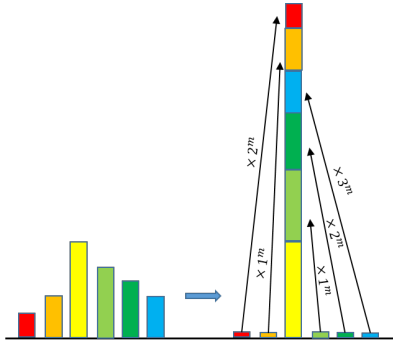


Figure 4: Optimal transport between model output probability mass function and a Dirac (one-hot) probability mass, using $d(i, j) = |i - j|^m$ cost.

while preserving its geometrical properties, see, for example, [Peyré *et al.*, 2019; Feydy *et al.*, 2019; Cuturi, 2013]. However, in the case where p is a Dirac point mass (i.e., having a one-hot probability mass function), solving equation (3) becomes trivial and becomes

$$OT(p, q) = \sum_{i=1}^k q_i d(i, j), \quad (4)$$

where j is the correct class, and k is the total number of classes, as is also depicted in Figure 4. Letting q denote a model’s output probabilities and p denote a one-hot target, equation (4) is of course differential with respect to the model outputs q and therefore can be used as a loss term for gradient-based optimization.

The cost metric d can incorporate domain knowledge in order to quantify the semantic distance between every two elements of M . Since in our case $M = \{1, \dots, k\}$ is an ordered space, a natural possibility is to define

$$d(i, j) = |i - j|^m,$$

for some $m \geq 1$, i.e., mapping the symbolic class labels to consecutive integers, and computing powers of absolute differences. When $m = 1$, the optimal transport can also be computed as the ℓ_1 distance between the cumulative mass functions², $\|\text{CMF}(p) - \text{CMF}(q)\|_1$, (see Levina and Bickel [2001], for example). This is equivalent to the computation in equation (4), and also generalizes to arbitrary targets (i.e., not necessarily Dirac).

4 The Proposed Approach

In this section we describe our proposed mechanism for architectural-based generation of unimodal output probability distributions.

4.1 Rational

The fact that the unimodality is obtained directly via architectural design has a major advantage over using soft targets for training, since the output probabilities are guaranteed to be unimodal for every input instance, as is also the case for

²This holds when the classes are ordered.

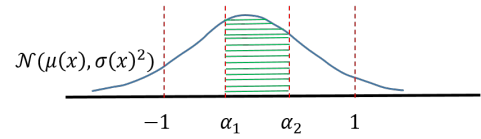


Figure 5: Generation of unimodal output probabilities for $k = 3$ classes. An input x is mapped to a (μ, σ) pair, which define a normal distribution $\mathcal{N}(\mu(x), \sigma(x)^2)$ over the real line. The output probabilities are proportional to the mass in the bins, which are of equal length. The green area equals to the unnormalized probability $\tilde{p}_2(x)$, corresponding to $\Pr(Y = 2|X = x)$.

the mechanism proposed by Beckham and Pal [2017]. However, unlike Beckham and Pal [2017], our proposed approach employs the normal distribution, depending separately on a location parameter and a scale parameter, so that the location of the mode is detached from the decay of the probability mass, which yields a more flexible design than the single-parameter distributions used by Beckham and Pal [2017], in which the single parameter determines both the mode and the decay. We will demonstrate in section 5 that this greater flexibility is helpful in expressing prediction uncertainty.

4.2 Unimodal Output Probabilities Generation

Inspired by the POM, we utilize thresholds to define bins, so that the total mass inside each bin is the output probability of the corresponding class. However, observe that the lack of unimodality of POM can be fixed by letting the bins be of equal length and remain fixed during training.

Therefore, instead of learning the thresholds, during training a map $x \mapsto (\mu, \sigma)$ is learned, where μ is a location parameter, and σ is a scale parameter, which define a $\mathcal{N}(\mu, \sigma^2)$ distribution, using which the output probabilities are computed.

Formally, we divide the range $[-1, 1]$ to k equal bins, where k is the number of classes, defined by $-1 = \alpha_0, \alpha_1, \dots, \alpha_k = 1$, so that $\alpha_i - \alpha_{i-1} = \frac{2}{k}$. The (unnormalized) probabilities are given by

$$\tilde{p}_i(x) = \Phi_{\mu(x), \sigma(x)}(\alpha_i) - \Phi_{\mu(x), \sigma(x)}(\alpha_{i-1}),$$

Where $\Phi_{\mu, \sigma}(\cdot)$ is the $\mathcal{N}(\mu, \sigma^2)$ cumulative distribution function, and we have emphasized that μ, σ are in fact functions of the input instance x . Since the bins cover $[-1, 1]$ and not the entire real line, we normalize the probabilities to obtain proper model predictions via

$$\Pr(Y = i|x) = p_i(x) \equiv \frac{\tilde{p}_i(x)}{\sum_{j=1}^k \tilde{p}_j(x)}. \quad (5)$$

To compensate for the fact that the probability generating mechanism depends on less parameters than POM (2 for the former, $d + k - 1$ for the latter), the map $x \mapsto (\mu, \sigma)$ is expressed via a deep network, which is therefore able to represent a complex nonlinear relation. Our proposed mechanism for generation of unimodal output probabilities is depicted in Figure 5.

The following lemma, proved in the appendix, establishes that the model output probabilities are indeed unimodal.

Lemma 4.1. *Let $x \in \mathbb{R}^d$ be an input to the model, which is mapped to $\mu = \mu(x), \sigma = \sigma(x)$, and let p_1, \dots, p_k be the*

model output probabilities, generated via equation (5). Then p_1, \dots, p_k define a unimodal multinomial random variable.

Proof. Let p_i, p_{i+1} be the output probabilities of two adjacent classes, and let $-1 = \alpha_0, \dots, \alpha_k = 1$ be the thresholds. We will show that (i) if $\mu \leq \alpha_{i-1}$ then $p_i \geq p_{i+1}$. Symmetrical argument will then imply that if $\mu \geq \alpha_{i+1}$ then $p_{i+1} \geq p_i$ (ii) if $\mu \in (\alpha_{i-1}, \alpha_i)$ then $p_i > p_{i+1}$, whenever the latter exists. Similarly, this would imply that $p_i > p_{i-1}$. Together, (i) and (ii) will imply the statement of the lemma.

Denote by f the density of the $\mathcal{N}(\mu, \sigma^2)$ distribution. To prove (i) observe that $\tilde{p}_i > \frac{2f(\alpha_i)}{k} > \tilde{p}_{i+1}$, which implies $p_i > p_{i+1}$.

To prove (ii), divide the i 'th bin to two sub-bins $B_{i,1}, B_{i,2}$, of lengths $a = \mu - \alpha_{i-1}$ and $b = \alpha_i - \mu$, respectively. Similarly, divide the $i+1$ 'th bin to two bins $B_{i+1,1}, B_{i+1,2}$ lengths b and a . Then from (i)

$$\int_{B_{i,2}} f(x)dx > \int_{B_{i+1,1}} f(x)dx. \quad (6)$$

In addition, observe that

$$\begin{aligned} \int_{B_{i,1}} f(x)dx &= \int_0^a f(\mu + x)dx \\ &> \int_0^a f(\mu + 2b + x)dx \\ &= \int_{B_{i+1,2}} f(x)dx. \end{aligned} \quad (7)$$

Adding up equations (6) and (7), we obtain $\tilde{p}_i > \tilde{p}_{i+1}$, which gives $p_i > p_{i+1}$. \square

We remark that all arguments made here with regard to the normal distribution also hold for other unimodal distributions, which are symmetric around μ , such as Logistic(μ, σ) and Cauchy(μ, σ), which both have slower decay patterns.

5 Experimental Results

To analyze the components of the proposed approach, we begin this section with small-scale ablation studies on the Abalone dataset. We then move to three larger real world datasets: Adience, Historical Color Images and Diabetic Retinopathy.

5.1 Ablation Studies

Here we use a modified version of the Abalone dataset³. The dependent variable counts the number of rings inside the abalone shell, corresponding to its age, which should be predicted from 8 numeric features. We slightly re-arranged the range of the dependent variable using a hand-crafted monotonic transform, resulting in a partition of the data to eight classes, with number of instances per class ranging between 391 and 689. The data file appears in our GitHub repository.

Table 1 shows the performance of our proposed approach, along with the following baselines:

- A neural network regression model, trained using squared error loss. The predicted class is obtained by rounding the model's (linear) output.
- A neural network classification model, trained using cross entropy loss and one-hot targets
- A standard POM.

In addition, to understand the contribution of the optimal transport objective and the unimodal probabilities mechanism, we also train two "hybrid" models:

- A neural network classification model, trained using optimal transport loss and one-hot targets (classification OT)
- A neural network model, with our proposed mechanism for unimodal output probabilities, trained using cross entropy loss, and one-hot targets (Unimodal CE)

All neural network models shared the same architecture, except for the output layer, and were trained using identical batch sizes and learning rate policies.

Method	MAE
Regression	1.00 ± .03
Classification	1.07 ± .04
POM	1.45 ± .03
Proposed	.97 ± .03
Classification OT	1.10 ± .01
Unimodal CE	1.12 ± .05

Table 1: Performance of various methods on the Abalone dataset, in terms of mean ± standard deviation over 5 independent trials.

Table 1 demonstrates a few interesting properties of the proposed approach. First, by analyzing the performance of the baseline models, we observe that the proposed approach significantly outperforms standard regression and classification, in terms of MAE. All three methods (the proposed, classification and regression) outperform POM on this dataset.

By looking at the performance of the hybrid models, we see that optimal transport objective, missing in Unimodal CE, and the proposed unimodal probabilities generation mechanism, missing in Classifier OT, both contribute to the performance. In addition, we observe that the optimal transport objective does not manifest its full advantage with softmax-generated probabilities, perhaps as softmax often yield a peaked probability mass function. Similarly, cross entropy seem to work better with standard softmax, comparing to our proposed unimodality mechanism. We observed these phenomena also in several other experiments, which are not described here.

Analysis of uncertainty Belharbi *et al.* [2019] claims that methods that learn a variance parameter may simply push it to zero, hence this parameter need to be manually set. We show that in our case, the learned map $x \mapsto (\mu, \sigma)$ does not yield a vanishing standard deviation parameter. Rather, the standard deviation corresponds to the uncertainty of the model in its predictions. To see that, we plot in Figure 6 the histograms of the probability of the mode of the predicted distribution (i.e., histograms of $\max\{p_1, \dots, p_k\}$), as a function of whether or not the mode predicts the ground truth class or not. As can

³<https://archive.ics.uci.edu/ml/datasets/abalone>

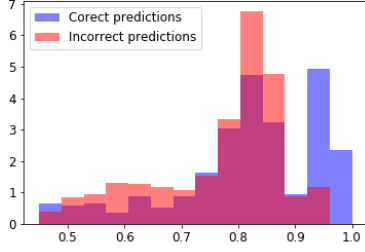


Figure 6: Histograms showing the probability of the mode of the output probabilities for Abalone test instances with correct and incorrect predictions

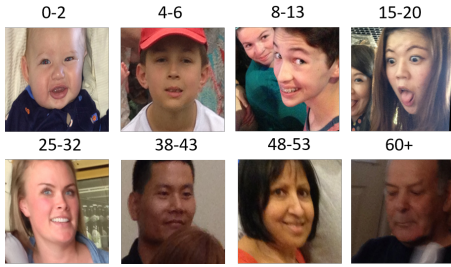


Figure 7: Examples from the Adience dataset. Age category is indicated above each image.

be seen, the modes are higher in cases of correct predictions, than in cases of incorrect predictions. Put another way, the prediction quality of the model has some consistency with the confidence. The higher the mode is, the more peaked the output probability function is, and the predictions indeed tend to be more accurate.

We now turn to experimental results on real world datasets

5.2 Results on Real World Datasets

Datasets

The Adience dataset⁴ contains 19,500 face images of 2,284 individuals. The label corresponds to the subjects' age group, out of 8 possible groups. Some examples from the dataset are shown on Figure 7.

The Historical Color Image (HCI) dataset [Palermo *et al.*, 2012] contains 1325 images, partitioned to 5 classes, corresponding to decades from 1930s to 1970s, and the task is to associate each images with the decade it was taken at. Some examples from this datasets are shown in Figure 8.

The Diabetic Retinopathy (DR) dataset⁵ contains 35,126 images of high-resolution retina images of 17,562 subjects, taken under a variety of imaging conditions. The images are labeled according to the presence of diabetic retinopathy. Some examples from this datasets are shown in Figure 9. We used the same pre-processing as Graham [2015].

⁴<https://talhassner.github.io/home/projects/Adience/Adience-data.html>

⁵<https://www.kaggle.com/c/diabetic-retinopathy-detection/data>



Figure 8: Examples from the HCI dataset. Decades categories are indicated above.



Figure 9: Examples from the DR dataset. DR classes are indicated above.

Methods Compared

We compare our proposed approach to four recently proposed approaches for deep ordinal regression, with unimodal output probabilities:

- DLDL [Gao *et al.*, 2017], an approach utilizing soft labels, generated using squared exponentially decaying distributions, trained using Kullback-Leibler divergence minimization (equivalent to cross entropy minimization).
- SORD [Diaz and Marathe, 2019], an approach utilizing soft labels, generated using linear exponentially decaying distributions, trained using Kullback-Leibler divergence minimization.
- [Beckham and Pal, 2017], architectural-based unimodal output probabilities, generated using binomial distribution (single-learned parameter), trained using optimal transport loss.
- [Liu *et al.*, 2019a], an approach utilizing soft labels, created as a mixture of Dirac, uniform and linear exponentially decaying distributions, trained using optimal transport loss.

In order to perform a fair comparison, we implemented all methods, using the same image transformations, backbone CNN and training procedures, so that the methods differ only in their output layer architectures and loss functions. We performed 5 independent trials, using the same train-validation-test splits for all methods. Additional technical details can be found in Section 5.2. For reproducibility, our GitHub repository <https://github.com/jsvir/unior> contains code reproducing all results reported in this section.

Results

Table 2 shows the test results of each method on the Adience, HCI and DR datasets. We report Mean Absolute Deviation (MAE), and percentage of test examples with unimodal predicted output probabilities. In addition, viewing the output probabilities as a multinomial distribution, we compare ratio

Dataset	Method	MAE	% Unimodal	avg entropy (incorrect predictions) avg entropy (correct predictions)
HCI	[Beckham and Pal, 2017]	0.7 ± 0.04	1 ± 0	0.99 ± 0.07
	[Liu <i>et al.</i> , 2019a]	0.56 ± 0.03	0.39 ± 0.03	0.8 ± 0.04
	[Gao <i>et al.</i> , 2017]	0.74 ± 0.03	1 ± 0	1.32 ± 0.14
	[Diaz and Marathe, 2019]	0.6 ± 0.02	0.96 ± 0.01	0.78 ± 0.07
	Proposed	0.6 ± 0.03	1 ± 0	1.83 ± 0.26
Adience	[Beckham and Pal, 2017]	0.52 ± 0.08	1 ± 0	1.16 ± 0.18
	[Liu <i>et al.</i> , 2019a]	0.48 ± 0.07	0.52 ± 0.02	1.08 ± 0.02
	[Gao <i>et al.</i> , 2017]	0.5 ± 0.06	0.62 ± 0.07	0.88 ± 0.16
	[Diaz and Marathe, 2019]	0.47 ± 0.07	0.99 ± 0	1.06 ± 0.03
	Proposed	0.44 ± 0.05	1 ± 0	2.01 ± 0.3
DR	[Beckham and Pal, 2017]	0.27 ± 0.01	1 ± 0	3.24 ± 0.21
	[Liu <i>et al.</i> , 2019a]	0.26 ± 0.01	0.91 ± 0.01	1.1 ± 0.01
	[Gao <i>et al.</i> , 2017]	0.26 ± 0.01	0.99 ± 0	1.73 ± 1.44
	[Diaz and Marathe, 2019]	0.27 ± 0.01	0.99 ± 0	1.12 ± 0.01
	Proposed	0.27 ± 0.01	1 ± 0	7.07 ± 0.62

Table 2: Performance of various methods on the HCI, Adience and DR datasets, in a mean \pm std format.

of the average entropy in correct predictions, to the average entropy in incorrect predictions.

On the HCI dataset, in terms of MAE, our proposed approach is outperformed by the method of [Liu *et al.*, 2019a]. Observe that despite the fact that this methods is trained with soft, unimodal targets, its output probabilities on test data is unimodal only 39% of the time. Similarly, SORD, which is also trained with soft targets, does not always output unimodal probabilities. Among the methods that output unimodal probabilities on this dataset ([Beckham and Pal, 2017], via architectural design and DLDL, via soft targets), the proposed approach is the best performing method.

On the Adience dataset, our method performs on the same level or better than all other methods in terms of MAE. Observe that on this dataset, [Beckham and Pal, 2017] and our proposed approach, both with architectural-based unimodality guarantee, are the only methods to always output unimodal probabilities.

On the DR dataset all 5 methods are comparable in terms of MAE. Here as well, the soft targets-based methods do not always output unimodal probabilities.

In addition, on all three datasets the ratio between average entropy of the output probabilities in correct prediction and the average entropy over incorrect predictions is significantly higher than the other methods. Similarly to Figure 6, this implies that the consistency between the shape of the output distribution and the quality of the prediction is stronger for our proposed approach comparing to the other baselines: the predictions tend to be more peaked when the decision is correct. We argue that this is a desired attribute of a probabilistic model.

Technical details

Table 3 shows the technical details for the experiments on the Adience, HCI and DR datasets.

In the DR experiment, all images of each subjects were contained in the same split (hence in each trial used either for training or for test, but not both). In the Adience experiment, we used the same train-test splits as the creators of the

	HCI	DR	Adience
Train images	1075	28,098	see below
test images	250	3512	see below
Backbone	ResNet18	ResNet18	ResNet101
Epochs	200	150	100
Batch size	16	128	64
Initial LR	1e-4	1e-4	1e-4
Decay LR after (epochs)	100	100	40
LR decay factor	0.1	0.1	0.01
Weight decay	1e-3	1e-4	1e-5

Table 3: Technical details for the HCI, DR and Adience experiments.

dataset⁶. The Adam optimizer was used in all experiments, with the default $\beta = (0.9, 0.999)$.

6 Conclusion

In this manuscript we presented an approach for deep ordinal regression, inspired by the proportional odds model, utilizing an architectural mechanism for generation of unimodal output probabilities, and trained using optimal transport objective. We empirically analyzed the components of the proposed approach, and demonstrated that they both contribute to the performance of the model. We demonstrated that while performing on-par with other recently proposed approaches for ordinal regression, our proposed method enjoys the benefits of guaranteed unimodal output probabilities, and of more significant difference in confidence between correct and incorrect predictions.

References

- Christopher Beckham and Christopher Pal. Unimodal probability distributions for deep ordinal classification. In *Proceedings of the 34th International Conference on Machine Learning-Volume 70*, pages 411–419, 2017.
- Soufiane Belharbi, Ismail Ben Ayed, Luke McCaffrey, and Eric Granger. Non-parametric uni-modality constraints

⁶https://github.com/GilLevi/AgeGenderDeepLearning/tree/master/Folds/train_val.txt.files_per_fold

- for deep ordinal classification. *arXiv*, pages arXiv–1911, 2019.
- Axel Berg, Magnus Oskarsson, and Mark O’Connor. Deep ordinal regression with label diversity. *arXiv preprint arXiv:2006.15864*, 2020.
- Jianlin Cheng, Zheng Wang, and Gianluca Pollastri. A neural network approach to ordinal regression. In *2008 IEEE International Joint Conference on Neural Networks (IEEE World Congress on Computational Intelligence)*, pages 1279–1284. IEEE, 2008.
- Marco Cuturi. Sinkhorn distances: Lightspeed computation of optimal transport. In *Advances in neural information processing systems*, pages 2292–2300, 2013.
- Raul Diaz and Amit Marathe. Soft labels for ordinal regression. In *Proceedings of the IEEE Conference on Computer Vision and Pattern Recognition*, pages 4738–4747, 2019.
- Jean Feydy, Thibault Séjourné, François-Xavier Vialard, Shun-ichi Amari, Alain Trounev, and Gabriel Peyré. Interpolating between optimal transport and mmd using sinkhorn divergences. In *The 22nd International Conference on Artificial Intelligence and Statistics*, pages 2681–2690, 2019.
- Huan Fu, Mingming Gong, Chaohui Wang, Kayhan Batmanghelich, and Dacheng Tao. Deep ordinal regression network for monocular depth estimation. In *Proceedings of the IEEE Conference on Computer Vision and Pattern Recognition*, pages 2002–2011, 2018.
- Bin-Bin Gao, Chao Xing, Chen-Wei Xie, Jianxin Wu, and Xin Geng. Deep label distribution learning with label ambiguity. *IEEE Transactions on Image Processing*, 26(6):2825–2838, 2017.
- Ben Graham. Kaggle diabetic retinopathy detection competition report. *University of Warwick*, 2015.
- Le Hou, Chen-Ping Yu, and Dimitris Samaras. Squared earth mover’s distance-based loss for training deep neural networks. *arXiv preprint arXiv:1611.05916*, 2016.
- Elizaveta Levina and Peter Bickel. The earth mover’s distance is the mallows distance: Some insights from statistics. In *Proceedings Eighth IEEE International Conference on Computer Vision. ICCV 2001*, volume 2, pages 251–256. IEEE, 2001.
- Yanzhu Liu, Adams Wai-Kin Kong, and Chi Keong Goh. Deep ordinal regression based on data relationship for small datasets. In *IJCAI*, pages 2372–2378, 2017.
- Xiaofeng Liu, Yang Zou, Yuhang Song, Chao Yang, Jane You, and BV K Vijaya Kumar. Ordinal regression with neuron stick-breaking for medical diagnosis. In *Proceedings of the European Conference on Computer Vision (ECCV)*, pages 0–0, 2018.
- Yanzhu Liu, Adams Wai Kin Kong, and Chi Keong Goh. A constrained deep neural network for ordinal regression. In *Proceedings of the IEEE Conference on Computer Vision and Pattern Recognition*, pages 831–839, 2018.
- Xiaofeng Liu, Xu Han, Yukai Qiao, Yi Ge, Site Li, and Jun Lu. Unimodal-uniform constrained wasserstein training for medical diagnosis. In *Proceedings of the IEEE International Conference on Computer Vision Workshops*, pages 0–0, 2019.
- Yanzhu Liu, Fan Wang, and Adams Wai Kin Kong. Probabilistic deep ordinal regression based on gaussian processes. In *Proceedings of the IEEE International Conference on Computer Vision*, pages 5301–5309, 2019.
- Xiaofeng Liu, Fangfang Fan, Lingsheng Kong, Zhihui Diao, Wanqing Xie, Jun Lu, and Jane You. Unimodal regularized neuron stick-breaking for ordinal classification. *Neurocomputing*, 2020.
- Frank Palermo, James Hays, and Alexei A Efros. Dating historical color images. In *European Conference on Computer Vision*, pages 499–512. Springer, 2012.
- Hongyu Pan, Hu Han, Shiguang Shan, and Xilin Chen. Mean-variance loss for deep age estimation from a face. In *Proceedings of the IEEE Conference on Computer Vision and Pattern Recognition*, pages 5285–5294, 2018.
- Gabriel Peyré, Marco Cuturi, et al. Computational optimal transport: With applications to data science. *Foundations and Trends® in Machine Learning*, 11(5-6):355–607, 2019.
- Vishnu TV, Pankaj Malhotra, Lovekesh Vig, Gautam Shroff, et al. Data-driven prognostics with predictive uncertainty estimation using ensemble of deep ordinal regression models. *arXiv preprint arXiv:1903.09795*, 2019.
- Víctor Manuel Vargas, Pedro Antonio Gutiérrez, and César Hervás-Martínez. Cumulative link models for deep ordinal classification. *Neurocomputing*, 2020.